# Ultraviolet Laser Ablation of Organic Polymers

R. SRINIVASAN* and BODIL BRAREN

*T. J. Watson Research Center, IBM Corporation, Yorktown Heights, New York 10598*

*Received August 2, 1988 (Revised Manuscript Received July 10, 1989)*

## Contents



## I. Introduction and History

During the 15-year period from 1960 when the very first laser was described to 1974 when the first excimer laser was built, the principal sources of laser radiation produced visible or infrared light. The output of some of these lasers could be multiplied in frequency to emit pulses of ultraviolet radiation but the energy output of these sources was too little (a few millijoules) to be useful in the study of the interaction of UV laser radiation with solid organic matter. In the mid-seventies, excimer lasers were invented almost simultaneously by several research groups. These lasers are powerful sources of pulsed, monochromatic ultraviolet laser radiation. Depending upon the gas fill, their output spans the entire UV wavelength range from 350 to 150 nm although the intensities are variable at the different wavelengths. Within a period of 3–5 years of their invention, excimer lasers with output pulses of 100–500 mJ and repetition rates of 200–500 Hz had become available commercially.

The interactions of laser pulses with organic matter have been investigated extensively over the past two decades. The use of infrared lasers gives rise to multiphoton excitation over the vibrational manifolds of ground electronic states which is then followed by thermal decomposition. The interaction of UV laser pulses with small polyatomic molecules has also received considerable attention following the early reports of Bernstein and co-workers[1] that in these molecules multiphoton excitation to upper electronic states results in ionization and decomposition by a variety of pathways.[2]

It was first reported in 1982[3,4] that when pulsed UV laser radiation falls on the surface of an organic polymer, the material at the surface is spontaneously etched away to a depth of 0.1 $\mu$m to several microns. The principal features of this phenomenon which readily distinguished the interactions of UV laser pulses from visible or IR laser pulses were the control that can be exercised over the depth of the etching by controlling the number of pulses and the fluence of the laser and the lack of detectable thermal damage to the substrate. The result is an etch pattern in the solid with a geometry that is defined by the light beam. Within a period of a year after the first report, other groups confirmed these observations in several other polymers and at different ultraviolet wavelengths.[5–8] The possibility of

R. Srinivasan is a native of Madras, India, and received his undergraduate education there. He obtained his Ph.D. from the University of Southern California under Dr. Sidney W. Benson. He did postdoctoral work at the California Institute of Technology and at the University of Rochester. He joined IBM's Thomas J. Watson Research Center in 1961 and is currently manager of a group on photochemical research. He has been a visiting professor at the City University of New York and The Ohio State University. He is currently a visiting research faculty member at the Columbia–Presbyterian Medical Center and at the Wellman Laboratory of Harvard Medical School. He is a Fellow of the New York Academy of Sciences and the American Association for the Advancement of Science and was a Guggenheim Fellow in 1965–1966.

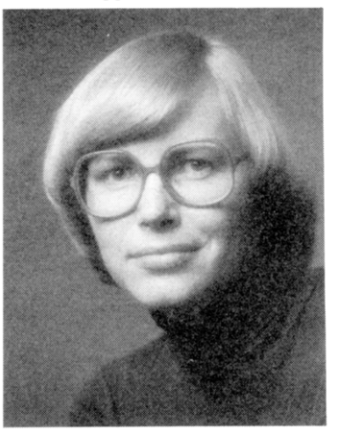

Bodil Braren was born in Denmark and educated in the areas of chemistry and physics. She is presently a staff engineer in the Physical Sciences Department at the Thomas J. Watson Research Center at IBM. Her work in the past 5 years has been focused on the understanding of the interaction of excimer lasers with materials.

0009-2665/89/0789-1303$06.50/0 

**TABLE I. List of Polymers Whose Ablation Interactions with Ultraviolet Laser Radiation Have Been Reported**

| polymer | ref[m] |
|---|---|
| poly(methyl methacrylate) (PMMA) | *a*, 7, 31, 33, 35, 44, 57, 62, 64, 77 |
| polystyrene | 19, 33, 45 |
| poly(α-methylstyrene) | *b* |
| nitrocellulose | 6 |
| pyromellitic dianhydride–oxydianiline condensate (Kapton) | *c*, *d*, 6, 15, 17, 18, 33, 36, 38, 39, 41, 54, 60, 75, 80 |
| poly(ethylene terephthalate) | *b*, *f*, 13, 20, 33, 54, 65 |
| bisphenol polycarbonate | *c*, *e*, *g*, 33 |
| polyethylene | *h* |
| polypropylene | *h* |
| poly(tetrafluoroethylene) (Teflon) | 63 |
| poly(phenylquinoxaline) | *i* |
| polyacetylene | *j* |
| poly(dimethylglutaramide) | 78 |
| chlorinated poly(methylstyrene) | 78 |
| poly(*N*-vinylcarbazole) | 77 |
| poly(cyclohexylmethylsilane) | *k* |
| poly[(*n*-butylphenyl)methylsilane] | *k* |
| poly(di-*n*-pentylsilane) | *k* |
| poly(dimethylsilane) | 24 |
| poly(dicyclohexylsilane) | 24 |
| poly(isopropylmethylsilane-*co*-*n*-propylmethylsilane) | *l* |

[a] Braren, B.; Seeger, D. *J. Polym. Sci., Polym. Lett.* **1986**, *24*, 371. [b] Burrell, M. C.; Liu, Y. S.; Cole, H. S. *J. Vac. Sci. Technol.* **1986**, *A4*, 2459. [c] Dyer, P. E.; Sidhu, J. *J. Appl. Phys.* **1985**, *54*, 7201. [d] Koren, G. *Appl. Phys. B* **1988**, *46*, 147. [e] Braren, B.; Srinivasan, R. *J. Vac. Sci. Technol.* **1985**, *B3*, 913. [f] Lazare, S.; Granier, V. *Appl. Phys. Lett.* **1989**, *54*, 862. [g] Lazare, S.; Soulignac, J. C.; Fragnaud, P. *Appl. Phys. Lett.* **1987**, *50*, 624. [h] Srinivasan, R.; Sutcliffe, E.; Braren, B. *Laser Chem.* **1988**, *9*, 147. [i] Lazare, S.; Granier, V. *Laser Chem.* **1989**, *10*, 259 [j] Golombok, M.; Gower, M. C.; Kirby, S. J.; Rumsby, P. T. *J. Appl. Phys.* **1987**, *61*, 1222. [k] Marinero, E. E.; Miller, R. D. *Appl. Phys. Lett.* **1987**, *50*, 1041. [l] Hansen, S. G.; Robitallie, T. E. *J. Appl. Phys.* **1987**, *62*, 1394. [m] In cases where one author has studied the same polymer more than once, only the most recent article is referenced.

extending the process to biological tissue was reported in 1983.[9]

Research devoted to understanding the science and developing the technology behind UV laser ablation of polymers has grown at a surprising rate over the past 7 years. A list of the polymers that have been studied along with leading references is given in Table I. The polymers poly(methyl methacrylate) (PMMA) (1) and poly(ethylene terephthalate) (PET) together with a polyimide that is the condensation product of pyromellitic dianhydride and oxydianiline (2) (commercial

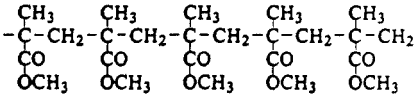

1

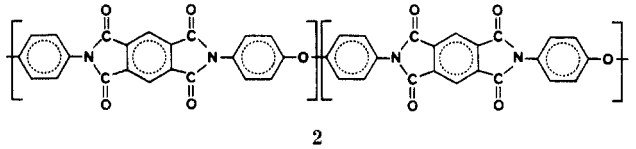

2

name for the film, Kapton) have received the lion's share of investigators' attention. All three of these polymers have attained considerable importance in electronics technology, PMMA and other acrylates as resist materials, polyimide as a dielectric, and PET as a base for tapes. It is technologically important to be able to pattern them. This is one of the principal reasons that UV laser ablation of polymers has attracted much research and development interest.

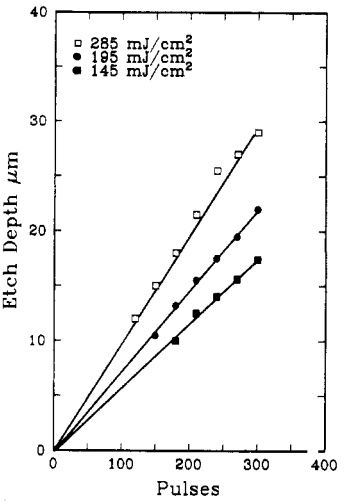


**Figure 1.** Etch depth as a function of number of pulses. Polyimide at 193 nm.

## *II. Characteristics of UV Laser Ablation*

Nearly all organic polymers show moderate to intense absorption in the ultraviolet region. These absorptions are usually ascribed to electronic transitions from a ground singlet to the first excited singlet states. The unique features in the UV laser ablation of polymers are encountered only in those wavelength regions in which such electronic absorptions exist.

The ablation of the surface of a polymer by a UV laser pulse is a function of the energy deposited in the solid in unit time. If a typical UV pulse has a full width at half-maximum (FWHM) of 20 ns and an energy of 450 mJ and the size of the beam at the polymer surface is 1.5 $cm^2$, the fluence at the surface will be 300 $mJ/cm^2$ and the power density will be $1.5 \times 10^7$ $W/cm^2$. When this pulse strikes the surface a loud audible report will be heard and, depending upon the wavelength, 0.01–0.1 μm of the material would have been etched away with a geometry that is defined by the light beam. If this experiment is performed in air, a bright plume will be ejected from the surface and will extend to a few millimeters. Typically, UV laser ablation is carried out with a succession of pulses. The etching of the surface with a train of uniform pulses is shown in Figure 1. The depth etched is a linear function of the number of pulses but note that there is a very long extrapolation between the origin (zero pulses) and the first data point. One can expect that at the first few pulses, the uniformity does not exist because the first pulse sees a virgin material whereas each subsequent pulse sees a sample that has already been modified in part by the preceding pulse. The slopes of the lines in Figure 1 give an average value for the etch depth/pulse at that wavelength and fluence for that material. These values are reproducible within the uncertainties in the measurement of the fluence of the laser and the depth of the etching.

Figure 2 shows a plot of the depth of etching per pulse vs the fluence at 193 nm for PMMA. In this and all subsequent discussion, although the fluence (number of joules per pulse/unit surface area of sample) is

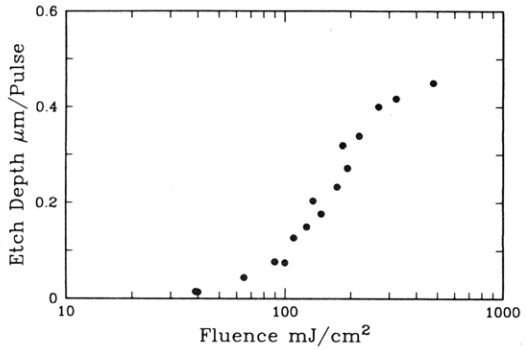


**Figure 2.** Plot of etch depth vs log (fluence) in laser ablation of PMMA at 193 nm.

quoted, one should keep in mind that it is the power density (power/unit area) that is important and discussions based on fluence are acceptable only so long as the pulse width is constant. Since the major portion of the data that are currently published and quoted in this review is based on pulse widths of 15–30 ns, this imprecision is not serious but nevertheless worth bearing in mind. The profile of the etch plot in Figure 2 is the typical "lazy S" form of a polymer with a moderate or weak absorption at the laser wavelength. There is always a threshold value for the fluence for the onset of etching and it is difficult to pinpoint this exactly because the etch curve approaches the abscissa asymptotically. This initial region of slight etching is followed by a steeply rising region in which the etch depth/pulse is linear with the fluence when the latter is plotted on a logarithmic scale. This linear region terminates in a third region in which the sensitivity of the polymer to etching rises more gradually or even decreases with increasing fluence. Usually, the absorption of the polymer decreases with increasing wavelength. The threshold fluence tends to increase with increasing wavelength and the linear portion increases in slope. Both the onset of etching and the flattening at high fluences become quite abrupt. It should be strongly emphasized that at a wavelength at which a polymer has no reported absorption (e.g., PMMA at 308 nm), etching does not decrease to zero. Instead, as the fluence is increased steadily, etching does set in but the two characteristics that are readily observable in UV laser ablation are no longer to be observed. These are the control that can be exercised over the depth of etching in a reproducible manner and the lack of thermal damage to the substrate. It is reasonable to say that at 308 nm, the characteristics of the etching pass over from photoablation to the thermal ablation that is observed at visible and infrared wavelengths.

## *III. Chemical Physics of the Ablation Process*

### A. Time Profile

A pictorial representation of the interaction of a laser pulse with a polymer surface is shown in Figure 3. As shown in Figure 3a, the stream of photons from a single laser pulse falls on the polymer and is absorbed in a depth that is defined by Beer's law. This depth can be as little as a fraction of a micron for intense absorbers to many tens of microns for weakly absorbing polymers. Obviously, weak absorption and strong absorption refer

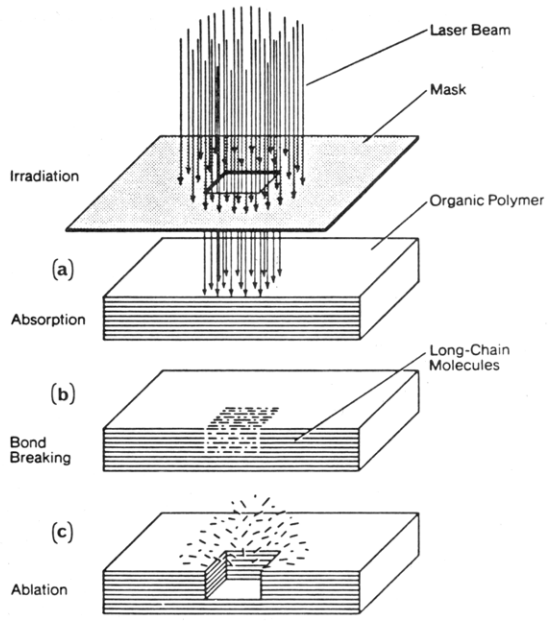


**Figure 3.** Schematic impact of laser pulse on polymer surface.

to specific wavelengths so that the same polymer can absorb weakly at one laser wavelength and strongly at another. Figure 3b shows that within the absorption depth, there are numerous bond breaks. In Figure 3c, the fragments are shown to be ejected from the surface, leaving an etched pit behind.

A knowledge of the timing of the ablation process is fundamental to an understanding of the chemical physics of the phenomenon. Early attempts to study it were based on a spectroscopic investigation of the light emission that accompanies the impact of a UV laser pulse on a polymer surface. Koren and Yeh[10,11] timed the intensity of the emission at various distances from the polymer surface and concluded that in the etching of polyimide films by 193-nm pulses (15-ns FWHM), the emission had a fast component that appeared simultaneously with the laser excitation, taking into account the ~30-ns response time of the photomultiplier used in the detection, but a slower component lasted 10–100-fold longer than the laser pulse itself. The emission from the plume in the ablation of PMMA at 193 nm (20-ns FWHM) was studied spectroscopically by Davis and co-workers,[12] who timed the peak in the intensity of the emission of CH radicals at various distances from the surface in order to calibrate its velocity of ablation. Their data also placed the beginning of the emission signal at times of the order of the width of the laser pulse. They pointed out that "it is possible that the photodissociation processes responsible for creating the emission in the plume are separate and subsequent to the breaking of the polymeric bonds which cause ablation". These two studies showed that the polymeric structure could begin to ablate on a time scale that is even shorter than the width of a pulse from the laser beam.

Dyer and Srinivasan[13] used the arrangement shown in Figure 4a[14] to measure the time profile of the ablation process in PMMA and other polymers. The film of PMMA (12 μm thick) was on a wide-bandwidth poly(vinylidene fluoride) (PVDF) piezoelectric transducer that, in turn, was pressure contacted with cyanoacrylate adhesive to a 4-mm-thick impedance-matching stub of

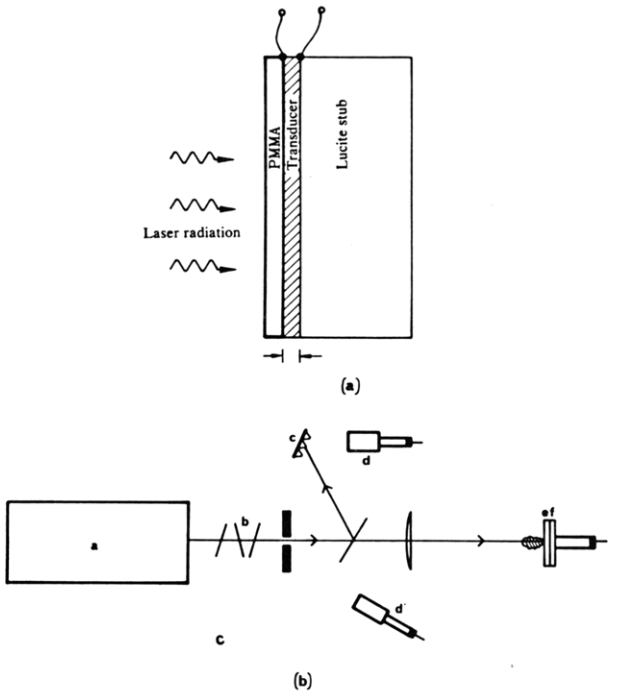


**Figure 4.** Photoacoustic measurements. (a) Arrangement of PMMA, transducer film, and lucite stub. (b) Experimental arrangement for recording stress wave and laser pulse in synchrony: (a) excimer laser; (b) attenuators; (c) scatterer; (d, d') silicon photodiodes; (e) PMMA; (f) PVDF transducer. Reprinted from ref 14; copyright 1987 Alan R. Liss, Inc.

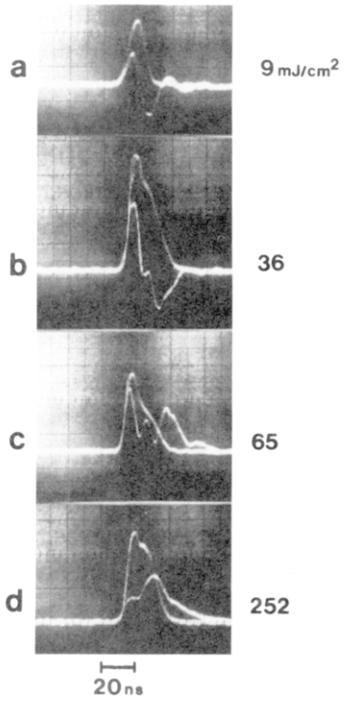


**Figure 5.** Time-synchronized laser and stress waveforms for laser-irradiated PMMA at 193 nm. The larger amplitude signal is the laser pulse that varies slightly in shape due to different operating voltages being used. Reprinted from ref 13; copyright 1986 American Institute of Physics.

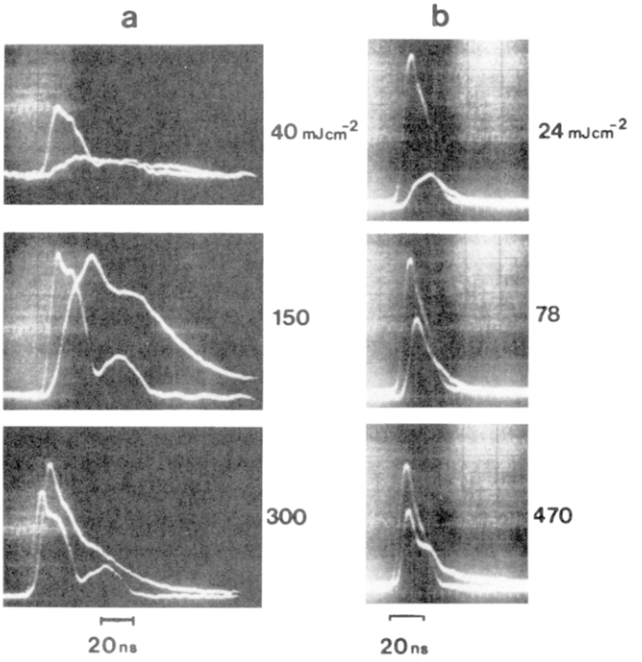


**Figure 6.** Time-synchronized laser and stress waveforms for polyimide film irradiated at various fluences: (a) 308-nm irradiation; (b) 193-nm laser irradiation. Reprinted from ref 13; copyright 1986 American Institute of Physics.

PVDF or PMMA. The latter minimized the acoustic reflection at the interface and gave a rise time limited by the transit time of the longitudinal wave in the transducer. When the electrical circuitry for the detection of the transducer signal was taken into account, the overall display system had a rise time that was estimated to be ≤5 ns. There is a time delay in the detection of the stress wave that is caused by its passage through the PMMA layer before it strikes the surface of the PVDF film. This delay can be measured in a separate experiment by measuring the transit time of an acoustic signal. The optical path of the laser beam to the silicon photodiode detector (Figure 4b) was adjusted so that the synchronization in the oscilloscope display of the start of the light pulse and the stress pulse referred to the front surface of the transducer was achieved to better than ±1 ns.

The local heating produced by a laser pulse at a fluence that is well below the threshold value at that pulse width causes a stress wave that is sinusoidal in character (Figure 5a). The compression wave caused by the heating is rapidly followed by a rarefaction wave caused by the cooling. As the fluence is increased, the onset of ablation is marked by a transition to an initially structured (Figure 5b,c) and then a relatively smooth compressive signal (Figure 5d). The last frame shows that when the fluence is sufficient to initiate strong ablation, the temporal width of the stress wave is about equal to that of the laser pulse and the point of initiation of both signals is nearly coincident.

Compressive stress signals from the irradiation of polyimide films with 193- or 308-nm laser pulses are shown in Figure 6. In this instance the stress wave due to ablation was observed to begin with a delay of ~4–6 ns after the start of the laser pulse. For the 16-ns (FWHM) 193-nm pulse, the duration of ablation (FWHM) as indicated by the stress pulse was 16–20 ns, whereas for the longer and more structured 308-nm pulse (~24 ns) the duration was 50–70 ns but decreased to ≤25 ns as the fluence increased above 200 mJ/cm². These compressive stress pulses persisted down to fluences well below the "threshold" fluence for etching that was determined from etch depth measurements.

The precision of these photoacoustic experiments depends upon the minimization of the rise time of the

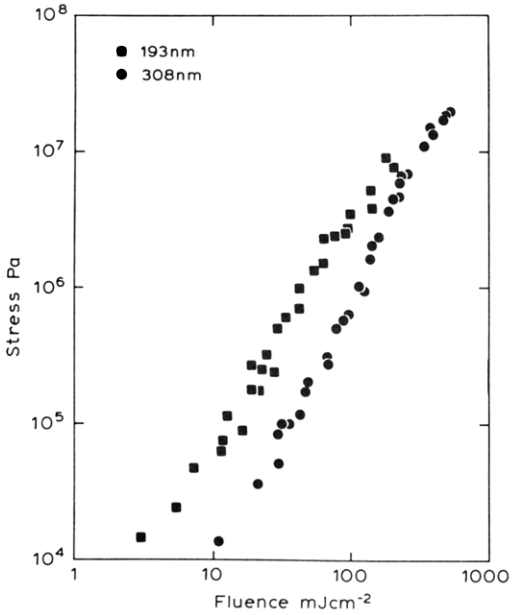


**Figure 7.** Peak amplitude of the stress wave as a function of fluence of polyimide film irradiatted with the 308- and 193-nm lasers. Reprinted from ref 13; copyright 1986 American Institute of Physics.

acoustic detector relative to the width of the laser pulse. For the same reason, the thickness of the polymer sample should also be small in order to keep the transit time of the stress wave to a minimum.

Particular note should be taken of the large magnitudes of the stress pulses that are generated in the ablation of both polymers by UV laser pulses. Figure 7 is a plot of the peak amplitude of the stress wave as a function of the fluence for the ablation of a polyimide film. The depth of the polymer that is etched is less than 1 $\mu$m per pulse at 193-nm wavelength. The ablated material is known to be ejected at 2–5 times the velocity of sound in air (vide infra). Therefore the pressure generated on the substrate is consistent with these measurements. It is interesting that this stress pulse extends even below the fluence at which significant etching is observed. Radicals and some ions are emitted at high velocity (which can be as large as $5 \times 10^5$ cm/s) at fluences at which the etch depth per pulse is below the limit for detection (about 500 Å even after 1000 pulses). The ablation of $\leq 5 \times 10^{-8}$ g of material at a velocity of $2 \times 10^4$ cm/s on a 20-ns time scale will account for the signal at 0.003 J/cm$^2$ in the interaction of 193-nm laser radiation with a polyimide film.

Simon[15] has recently photographed the surface of a polyimide film undergoing ablation with a 308-nm, 30-ns full-width pulse by the use of a visible probe beam of about 250-ps duration at 580 nm. His results are shown in Figure 8. It is evident that at the lowest fluence of 0.3 J/cm$^2$, ablation begins in 8 ns and continues up to 28 ns. The increasing depth of the etched spot can be seen as a function of time, which suggests that ablation proceeds layer by layer. The first sign of etching occurs earlier in time as the fluence is progressively increased to 1.1 and 4.0 J/cm$^2$. On the basis of this work and the photoacoustic studies, the pictorial representation in Figure 3b,c should be modified.

Acoustic signals from polymer films from the impact of UV laser radiation at even lower fluences (<0.0001 J/cm$^2$) have been recorded by Gorodetsky et al.[16] In

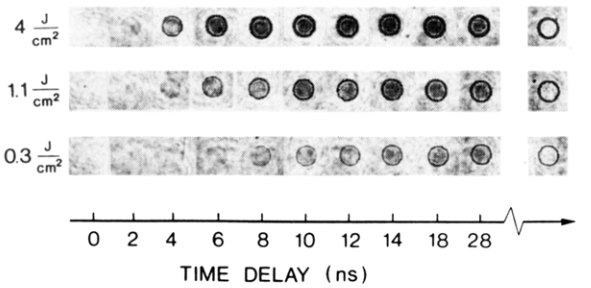


**Figure 8.** Ultrafast (<1 ns) photography of ultraviolet (308 nm) laser ablation of polyimide. At each of three fluences indicated on the left, a series of photographs of the ablating surface was taken with a fast, subnanosecond visible laser pulse. The progress of the etching during a single UV pulse of ~30-ns full width is evident. Reprinted from ref 15; copyright 1989 Springer-Verlag New York, Inc.

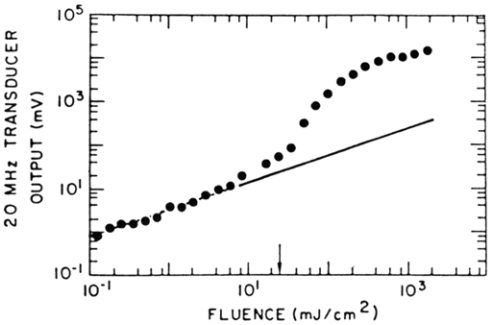


**Figure 9.** Acoustic signal vs laser fluence at 193 nm. An abrupt increase is detected at the ablation threshold. Reprinted from ref 16; copyright 1985 American Institute of Physics.

these experiments, the aim was not to resolve the time profile of the acoustic signal but merely to measure its magnitude as a function of the fluence of the beam. There is an increase in the acoustic signal (Figure 9) at the fluence at which etching can be first observed but the exact value of the so-called "threshold fluence" is seen to be as difficult to determine from acoustic data as from data on etching. The polymer that was used in this study was also polyimide. There appears to be a definite relationship between the chemical structure of a polymer and its acoustic behavior in the fluence range that lies well below the threshold for etching. For example, in the case of PMMA, which is a weakly absorbing polymer, Figure 5a shows that a laser pulse at 0.009 J/cm$^2$ (193 nm) gives a sinusoidal response, which is in contrast to the behavior of polyimide.

## B. Ablation Products

A knowledge of the composition of the material that is ablated from the surface of a polymer is of importance in understanding the chemistry of the process. It is also of potential use in the design of a UV laser tool for technology that can ablate a given surface most economically and with the least damage to the sample.

Chemical analysis of the ablation products has not received as much attention as physical aspects of ablation. This can be attributed to a number of difficulties, which include the following:

(i) Systems in which the ablation products have been collected and analyzed show that the products range from atoms and diatomics to volatile polyatomic molecules of low molecular weight (<200 mass units) to fragments of the polymer (up to molecular weight 10 000). Such a complex mixture of materials cannot

be readily analyzed by a single analytical technique.

(ii) There is evidence that the composition of the products changes with the UV wavelength used, the repetition rate of the pulses (since this will affect the dissipation of any heat energy that is left in the substrate from one pulse to the next), the chronology of the pulses (since the first 1–100 pulses may not etch in the same manner as when the system settles down to a constant etch depth/pulse at a given fluence), and the absolute fluence value (since with increasing fluence, the initial products of ablation can be decomposed further by incoming photons).

(iii) While the etch depth/pulse may not be sensitive to the pressure of air at the polymer surface, the products almost certainly undergo reaction with the oxygen and the nitrogen in the air.

(iv) The net quantity of products that is formed is of the order of only milligrams in typical experiments on a laboratory scale. This, when combined with the complexity of the products referred to in (i) above, increases the difficulty in the analysis.

Commercial polymers contain various additives that are meant to improve their physical and chemical properties. They also contain residual monomers, catalysts, and impurities. While polymers that are free from these contaminants can be prepared and used in research, the data that are so obtained may not be easy to relate to data that are obtained from commercial samples; i.e., the impurities in the commercial samples may contribute to their laser ablation behavior.

The products of ablation can be classified into several categories according to their morphology and molecular weight. The analytical methods to detect them have been selected in relation to these properties. It is obvious that certain methods (e.g., infrared spectroscopy) are more widely applicable than others.

The first category consists of volatile stable compounds usually of molecular weight <200. They have been analyzed by mass spectroscopy. While the mass spectral technique is capable of high sensitivity (picogram levels), a quantitative estimate of one component in a mixture of many products, all of which are not fully characterized, is not easy. It is more practical to use a combination of a gas chromatograph and a mass spectrometer to conduct a separation of the product mixture into its components and then measure each component quantitatively. This has been done in the cases of two polymers. Not only is this technique tedious but it also requires considerable effort to obtain the maximum sensitivity.

The second category, which is also the major weight fraction of the ablation products in many instances, is found as solid material. Following its expulsion into the atmosphere, a part of this fraction settles on the sides of the etched surface. If the ablation is carried out in a closed vessel under a vacuum, this product can travel as much as 10 cm before settling down on the window and on the inner walls of the irradiation cell. This material can be collected and analyzed by standard chemical methods. To make the collection more exhaustive, the irradiation of polyimide film was carried out under a millimeter layer of water by Srinivasan, Braren, and Dreyfus.[17] The solid product, which, in this case, is carbon, formed a colloidal suspension in the aqueous medium, while HCN, which is another significant product, dissolved in the water.

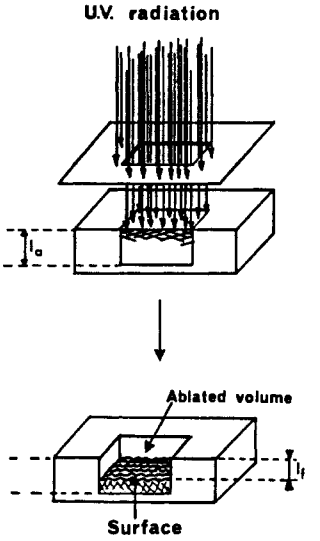


**Figure 10.** Schematic impact of several laser pulses on a polymer surface.

Optical spectroscopy has been used by several groups for the detection of transient species such as atoms and diatomics, which form the third category of products. Initial experiments were based on the emission spectrum from the species. It has been pointed out that the excited diatomic species that is the source of light emission may be formed by a secondary photolysis of an initially formed product.[18] Thus, absorption spectroscopy would be a more fundamental method to probe for transient species in the plume. Laser-induced fluorescence spectroscopy (which is discussed in the next section), which combines absorption spectroscopy with fluorescence detection, has been successfully used to probe for transient species such as $C_2$ and CN in the laser ablation of several polymers.

While at first sight it may seem as if information about the chemistry of the ablated material can be gathered only by analyzing the plume itself, information can also be obtained indirectly by a study of the surface that is created by ablation, which is the fourth category of products. This is shown by the shaded area in Figure 10. The shading represents a section of the volume that has already been transformed by the last one or few pulses and will be ablated by the next pulse. Its chemistry is therefore a precursor to the processes that will occur in the plume on actual ablation. At a resolution down to 1 $\mu$m, this surface has been examined by scanning electron microscopy (SEM) and optical microscopy. This helps to see if the bottom of the etched pit is smooth or convoluted and whether it is marred by melting and/or gas evolution or not. It is also useful for observing the deposition of solid debris in and around the etch pit. For information at an atomic level, X-ray photoelectron spectroscopy has been used with considerable success. This gives information on the chemical composition in the first 100 Å of depth of the etch pit. This technique has served to demonstrate that, after the first laser pulse, the composition of the polymer surface is permanently altered at least to a depth of 50–100 Å.[19–23] This information is corroborated by the measurement of the contact angle for water at the new surface. Rutherford back-scattering is another technique of use in the study of the compo-

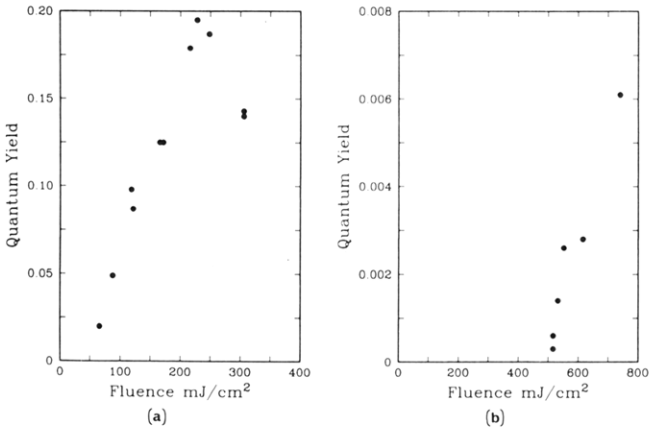


**Figure 11.** Quantum yields of monomer in laser ablation of PMMA: (a) at 193 nm; (b) at 248 nm. Reprinted from ref 30; copyright 1986 American Chemical Society.

sition of the etched surface.

Table II summarizes the data that are currently available on the products of the ablation of several polymers by UV lasers. While there is a great deal of qualitative information, the amount of quantitative information that correlates the yield of a given product to the mass of the polymer that was removed by ablation is sparse. The three polymers about which some detailed data are available are discussed here as they may be prototypes of the response of all-carbon chain polymers to UV laser radiation. Polysilanes fall in a class by themselves in their response to UV laser radiation. Recently, as a result of an elaborate and painstaking analysis of the products of the laser irradiation, it has been possible to draw significant conclusions about the modes of break up of these polymers under both UV and infrared laser pulses.[24-29] The reader should refer to the original articles (especially ref 24) for further information.

*PMMA.* The starting material is a commercial sample of $\bar{M}_n \sim 10^6$. The most important stable products in the gas phase are CO, $CO_2$, and the monomer, methyl methacrylate (MMA). The quantum yields at 193 and 248 nm are shown in Figure 11.[30] Since the absorption coefficient for this polymer at 248 nm compared to 193 nm drops by 1 order of magnitude, the quantum yields, which are calculated from the total number of photons absorbed, are not so useful as the chemical yield, which relates the yield of MMA at a particular fluence to the mass of the polymer that was ablated at the same fluence. These values are 18% and 1%, respectively, at 193 and 248 nm. There are not quantitative data on the yield of solid polymer that was ejected. Solubility tests placed the average molecular weight of the product obtained at 193 nm to be smaller than the value of $\bar{M}_n$ = 2500 for the product obtained at 248 nm. The morphologies of the ablated polymer and of the etched surfaces are shown in Figures 12 and 13. They convincingly demonstrate that the local temperature in the etched volume is greater than the melting point of PMMA (about 150 °C) during ablation with 248-nm laser pulses but not with 193-nm laser pulses, both at a fluence that is close to the ablation threshold. The data on the transient species, $C_2$, in this system will be discussed in the next section.

An interesting perspective on the photochemistry of this material is brought out by the study of Estler and

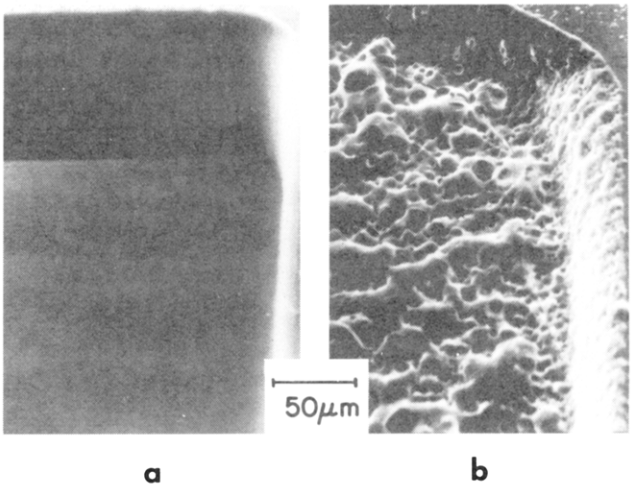


**Figure 12.** SEM photographs of the inside surface of etch pits of PMMA: (a) 193 nm, fluence of 0.70 J/cm²; (b) 248 nm, fluence of 2.70 J/cm². Reprinted from ref 30; copyright 1986 American Chemical Society.

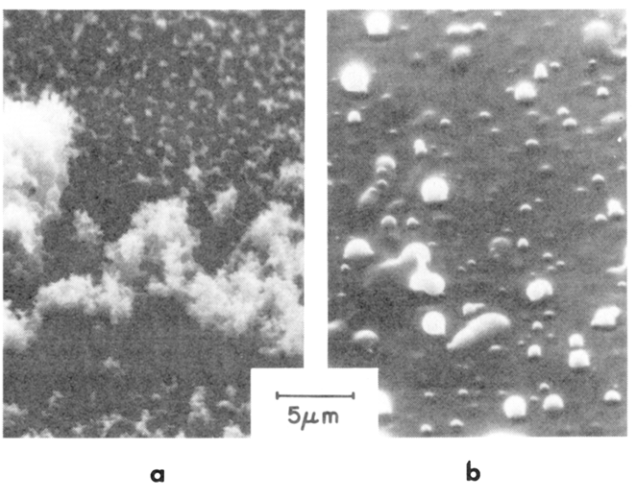


**Figure 13.** SEM of solid material ejected during laser irradiation of PMMA: (a) 193 nm, fluence of 0.15 J/cm²; (b) 248 nm, fluence of 2.70 J/cm². Reprinted from ref 30; copyright 1986 American Chemical Society.

Nogar.[31] These workers analyzed the volatile products of the interaction of PMMA with UV laser pulses by mass spectroscopy. At 266 nm and a fluence of 0.05 J/cm², they observed CO, $CO_2$, and MMA. But at a laser wavelength of 240 nm, at a comparable fluence, they found only CO and $CO_2$ but not MMA. Instead they observed the formation of methyl formate, which is a major product of the one-photon photochemistry of PMMA.[32] They conclude that they are irradiating the polymer at wavelengths at which the fluences that they used are insufficient to lead to two-photon excitation. This work demonstrates that in polymer–UV laser pulse interactions, there can be very different decomposition pathways that are not only wavelength dependent (a concept that is easily understood) but also dependent upon the photon multiplicity.

Kuper and Stuke[33] have characterized the sites in the polymer that are the first to be chemically transformed by UV laser radiation by the use of Fourier transform infrared spectroscopy. They have also shown that the absorption characteristics of the film in the ultraviolet undergo a change as it is ablated by a UV laser pulse at 248 nm.[34] This result has been independently shown

**TABLE II. Chemical Composition of Ablated Material**

| no. | polymer | sample characteristics | laser wavelength, nm | exptl conditions | ablated products: monomer or smaller | ablated products: larger than monomer | substrate anal. and morphology | anal. methods | ref[a] |
|---|---|---|---|---|---|---|---|---|---|
| 1. | PMMA (poly(methyl methacrylate)) | (i) fee standing; various molecular weights from 13 700 to $10^6$ | 193 nm | 0.04–18.0 J/cm$^2$ | C (a)[a]<br>$C_2$ (a, b) | polymer (e, f) ($\bar{M}_n$ = 2500, 248 nm; | no change in atomic composition of first | emission spectroscopy (a) laser-induced | A, B, 12, 31, 35, |
| | | | 222 | 0.05–??? J/cm$^2$ | CN (a) | $\bar{M}_m$ = 4500, 248 | 100 Å (i); change in | fluorescence (b), | 44, 46, |
| | | | 248 | 0.15–10.0 J/cm$^2$ | CN[b] (a) | nm); no sign of | UV absorption (j); | mass spectroscopy (c), | 57, 65 |
| | | (ii) spun film on neutral substrate | | | CO (c) | melting at 193 nm | no thermal damage | gas chromatography | |
| | | | 308 | 0.50–3.0 J/cm$^2$[c] | $CO_2$ (c) | at 10-W fluence | (melting, charring) | (d), gel permeation | |
| | | | (FWHM = 5–30 ns) | air atmosphere or vacuum | MMA (methyl methacrylate) (c, d) | (g); melting at high fluence at 193 nm and at all fluences | at 193 nm at 10-W fluence (see Figure 12); melting and | chromatography (e), infrared spectroscopy (f), scanning electron | |
| | | | | repetition rate <10 Hz | methyl formate (c) | at 248 nm | bubbling at 248 nm (g, h) | microscopy (g), optical microscopy (h), X-ray photoelectron spectroscopy (XPS) (i), ultraviolet spectroscopy (j) | |
| | | | | 90–293 K (external temperature) | | | | | |
| 2. | polystyrene | (i) free-standing low density (0.04–0.14 g/cm$^2$) | 193 | <1 J/cm$^2$, air atmosphere | styrene (c) | carbon (k)<br>polystyrene (a, i) | | Raman spectroscopy (k) | A, C, 33, 45 |
| | deuterated polystyrene | (ii) high density | 248 | | | | | | |
| 3. | poly($\alpha$-methyl-styrene) | spun on neutral substrate | 193 | <0.5 J/cm$^2$, air atmosphere | | | partial loss of aromatic rings in surface (i) | | |
| 4. | nitrocellulose | nitrocellulose linen fiber, 13.2% N | 193 | 0.02–0.20 J/cm$^2$ | gaseous products (c) | none | <3 nm of residue at 193 nm; more residue at longer wavelengths (g) | emission spectroscopy (a), laser-induced fluorescence (b), mass spectroscopy (c), gas chromatography (d), scanning electron microscopy (g) | D, 5, 6 |
| | | spin film on neutral substrate | 351 FWHM = 5–30 ns | | | | | | |
| | | | 308 | 0.10–3.00 J/cm$^2$ | $CO_2$ (c) | | | | |
| 5. | polyimide (Kapton) | (i) PMDA-ODA[d] spin coated as polyamic acid solution and cured | 193 | 0.02–9.0 J/cm$^2$ | C I (a)<br>C II (a) | carbon solid (f, g) polymer (f–h) | blackening (h); O/C ratio decreased by 12% (c); carboxylic group decreased by 40% (i) | infrared spectroscopy (f), optical microscopy (h), X-ray photoelectron spectroscopy (XPS) (i) | 10, 11, 17, 18, 23, 36, 38, 39, 42 |
| | | | 248 | 0.07–5.0 J/cm$^2$ | $C_2$ (a, b) | | | | |
| | | (ii) free-standing film (Kapton) | | | CO (f) | | | | |
| | | | 308 | 0.05–2.0 J/cm$^2$ | $CO_2$ (f) | | | | |
| | | | 351 | 0.10–15 J/cm$^2$ | $H_2O$ (f)<br>HCN (f) | | | | |
| | | | (FWHM = 7–30 ns) | air atmosphere vacuum, or water; repetition rate <10 Hz | benzene (c, d) | | | | |
| 6. | Mylar PET (poly(ethylene terephthalate)) | free-standing film, 1.7 mil thick | 193 | 0.03–0.50 J/cm$^2$ | $H_2$ (c) | solid polymer (g, h) | O/C ratio drops from 1.2 to 0.7 at surface (i) | contact angle measurement (k) | E, 22, 37 |
| | | | 248 | 0.20–2.00 J/cm$^2$ | CO (c) | | | | |
| | | | 308 | 0.10–3.00 J/cm$^2$ | $CO_2$ (c) | | surface hydrophilic (k) | | |
| | | | FWHM = 7–30 ns | repetition rate <10 Hz | $C_2$–$C_{12}$ (numerous products (c)) | | corrugated surface (g) | | |
| | | | | | benzene (c) | | | | |
| | | | | | toluene (c) | | | | |
| | | | | | benzaldehyde (c) | | | | |
| 7. | polyorganosilane various compositions | spin coated (see ref 24) | multiphoton excitation at 532 or 626 nm; also 308 nm | power density >2.5 GW/cm$^2$ FWHM = 4–6 ns | see ref 24 for mass spectral analysis | | | ultraviolet spectroscopy (j), mass spectroscopy (c) | F, G, 24, 25, 26, 27, 28, 29 |
| | D- and $^{13}$C-labeled polyorganosilanes | | | 0.15–0.25 J/cm$^2$ at 308 nm | | | | | |

[a] For ref a–k, see Table I. Additional references: (A) Burrell, M. C.; Liu, Y. S.; Cole, H. S. *J. Vac. Sci. Technol.* **1986**, *A4*, 2459. (B) Braren, B.; Seeger, D. *J. Polym. Sci., Polym. Lett.* **1986**, *2*, 371. (C) Hargis, P. J. *Am. Inst. Phys. Conf. Proc.*, in press. (D) Geis, M. W.; Randall, J. N.; Deutsch, T. F.; DeGraff, P. D.; Krohn, K. E.; Stern, L. A. *Appl. Phys. Lett.* **1983**, *43*, 74. (E) Lazare, S.; Soulignac, J. C.; Fragnaud, P. *Appl. Phys. Lett.* **1987**, *50*, 624. (F) Marinero, E. E.; Miller, R. D. *Appl. Phys. Lett.* **1987**, *50*, 1041. (G) Marinero, E. E. *Chem. Phys. Lett.* **1985**, *115*, 501. [b] An artifact produced by reaction of ablation products with atmospheric nitrogen (49). [c] No etching except at high (>20 Hz) repetition rate. [d] Condensate of pyromellitic dianhydride and oxydianiline.

to be measurable at 193, 222, and 248 nm as well by Davis and Gower.[35]

*Polyimide (PMDA-ODA).* The structure of this polymer is such that, as indicated (2), it can readily fragment to gaseous products such as HCN, CO, $C_2H_2$, etc. Early work on product analysis,[18,36] when compared to the products of pyrolysis,[37] gave rise to confusing interpretations. Recent work using an ion cyclotron resonance spectrometer[38] has successfully sorted out the ionic species formed in the plume. These are a minor part of the product mixture and they consist largely of clusters of carbon atoms (up to 800 amu) which may have come from the clustering of relatively small fragments such as $C_1$, $C_2$, and $C_3$. The neutral part of the ablated material has been analyzed also by mass spectrometry using a second laser to ionize the species by multiphoton ionization.[39] This study has given a more complete picture of the composition of the ablated material. Not only were clusters up to 1600 amu detected but these were not wholly attributed to carbon clusters. The composition of the products was influenced by the ablation fluence. The solid product that collects on the ablated surface around the area that is exposed to light has been identified as largely, if not exclusively, carbon.[17] Its charged nature has been reported.[40] Both its distribution on the surface as a function of ablation conditions[41] and its elimination due to oxidation by oxygen in the atmosphere[42] have been studied. The deposition of carbon particles on the ablated surface is a problem of practical interest.[43]

## C. Fate of the Ablated Material

When a UV laser pulse impinges upon a polymer surface, the etched material is ejected from the surface with considerable velocity and directionality. The dynamics of this plume has been the subject of much research.[12,17,30,44-53]

The velocities of specific molecules in the stream and their angular distribution have been determined. From the distribution of the velocities, a translational temperature has been estimated for the species. This temperature has been compared to the vibrational-rotational temperature which can be calculated for the same or other specific molecules in the plume from their spectra. The total momentum of the ejected material has been estimated. The velocity and angular distribution have been estimated for a hypothetical polymer whose ablation behavior has been modeled.

One example each of an investigation in which each of the following methods of detection were used will be described in detail: laser-induced fluorescence (LIF), mass spectrometry, and emission spectroscopy.

LIF is an analytical method of high precision that is suitable for the measurement of a specific diatomic species in the plume. The geometry that was used[18,45,54] is shown in Figure 14. The plume was probed by a dye laser beam at a distance from the surface of the polymer that was large enough to avoid any interference from the background luminescence at the film surface during ablation. The laser wavelength was 248 nm. The UV pulses were repreated at 5 Hz, and the polymer was slowly translated past the UV beam. Following a UV laser pulse, after a preset time delay, a probe pulse was fired from the dye laser at the plume. The wavelength of the probe pulse was sufficiently narrow to excite only

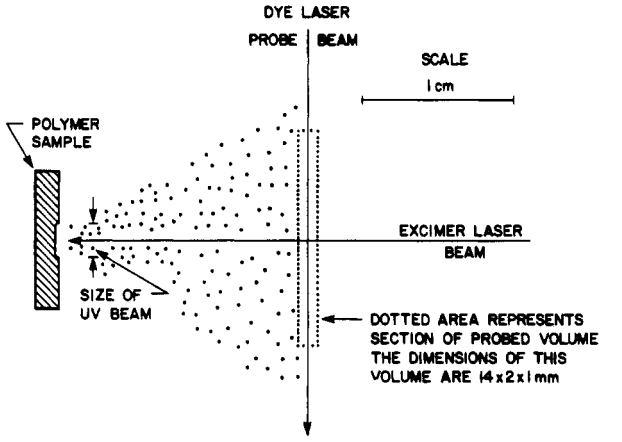


**Figure 14.** Geometry of UV laser beam and fluorescence pump beam with respect to polymer sample and fluorescence detection system. Reprinted from ref 17; copyright 1987 American Institute of Physics.

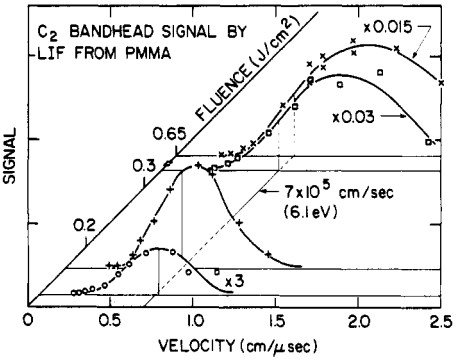


**Figure 15.** LIF signal from $C_2$ radicals indicating the distributions in velocities. Laser irradiation of PMMA at 248 nm. Reprinted from ref 30; copyright 1986 American Chemical Society.

one predetermined transition in the diatomic product that was being monitored. The fluorescence that the excited product then emitted was detected and analyzed quantitatively. Since the time delay between the excimer laser pulse and the dye laser pulse could be varied, the intensity (=concentration) of the diatomic product in the volume of the plume that was being probed could be determined at various times after the start of the UV pulse that caused the ablation. The time delays that were set were of the order of microseconds so that the width of neither the UV pulse nor the dye laser pulse introduced any significant error in the timing. From these data, information could be derived on the velocity distribution of the diatomic species in the plume at a particular UV laser fluence. A typical set of curves for the $C_2$ bandhead signal in the ablation of PMMA at 248 nm is plotted as a function of fluence in Figure 15. The probing wavelength of the dye laser corresponded to 438.2 nm [(2,0) of the $d^3\Pi_g \leftarrow a^3\Pi_u$ transition] and the detection wavelength of 471.5 nm corresponded to (2,1) in the same transition. The most surprising feature of these data is that while the intensities of the fluorescence signal changed by a factor of 200 as the fluence increased from a value (0.15 J/cm$^2$) that is lower than the threshold for ablation to a valeu (0.65 J/cm$^2$) well above it, the maximum velocity changed by only about 30%. It indicated that the production of $C_2$ and its ejection at a supersonic velocity of $7 \times 10^5$ cm/s took place even at a fluence at which etching of the surface of the polymer was too

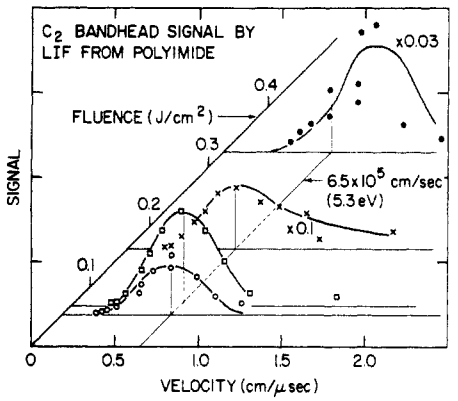


**Figure 16.** Velocity measurements on $C_2$ fragments from the ablation of polyimide at 248 nm. Reprinted from ref 17; copyright 1987 American Institute of Physics.

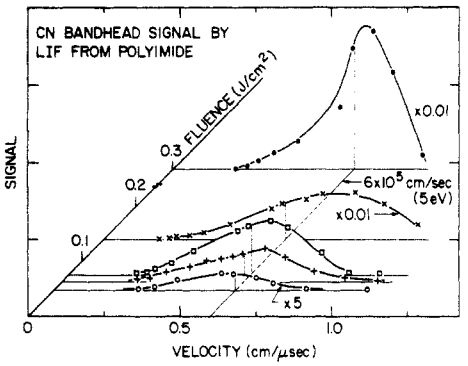


**Figure 17.** Velocity measurements on CN fragments from the ablation of polyimide at 248 nm. Reprinted from ref 17; copyright 1987 American Institute of Physics.

little to be measured by a surface profilemeter. An examination of the structure of PMMA shows that the pair of carbons that are likely to be the source of $C_2$ are a pair situated along the polymer chain (1) and the number of bonds to be cleaved to form it and eject it at the velocity mentioned above (= 6.1 eV) would require 3 photons of 248-nm (=5 eV) wavelength. This is perhaps the most direct evidence that multiphoton photochemistry is important in the ablation of polymers by UV laser radiation.

Velocity measurements on $C_2$ and CN fragments from the ablation of polyimide films with 248-nm laser radiation are shown in Figures 16 and 17. In an attempt to fit the velocity distribution of $C_2$ to a Maxwell–Boltzmann distribution it was found[17] that the measured points are narrowed with respect to the calculated curve. Such a result can be anticipated if the vaporization is not into a freely expanding gas phase but into a dense colliding medium. This medium is visualized as expanding subsequently into the requisite diffuse gas. One outcome of this picture is that true vaporization occurs not in the laboratory rest frame of reference but in a moving center-of-gravity frame which has been discussed elsewhere.[55] The cosine function, usually associated with effusion or vaporization appears as a narrowed distribution because the LIF measurement is made in the fixed laboratory frame. To some degree the velocity/angular dependence in this experiment can be viewed as a supersonic expansion; i.e., the velocity is peaked in the forward direction and therefore the velocity distribution is somewhat narrower than a Maxwell–Boltzmann distribution. The data points can

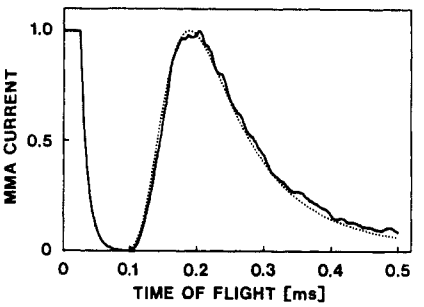


**Figure 18.** Velocity measurements on MMA (methyl methacrylate) from the ablation of PMMA at 193 nm. The dotted line corresponds to a Maxwell velocity distribution with a temperature $T$ = 1200 K. Reprinted from ref 44; copyright 1986 American Institute of Physics.

be better fit by a Boltzmann curve plus a constant additive velocity which represents the motion of the center of gravity. These results should be contrasted with velocity measurements obtained by the same technique on the UV ablation of graphite and sapphire.[56]

Velocity measurements on the stable polyatomic product methyl methacrylate (MMA) from the ablation of PMMA by 193-nm laser photons have been made by Danielzik et al.[44] by a different detection method. In their work, the ablation products were directed to the entrance slit of a quadrupole mass spectrometer (QMS) in which they were ionized and mass analyzed. The most common product that was encountered at fluences <0.2 J/cm$^2$ was MMA, and its velocity distribution at a fluence of 0.08 J/cm$^2$ is shown in Figure 18. The signal for times <50 μs is due to scattered light leaking into the QMS detector. The signal at later times ($t$ > 100 μs), which represents the actual MMA current, corresponds well to a Maxwell–Boltzmann distribution at a temperature of 1200 K. At all fluences < 0.15 J/cm$^2$, the measured velocity distributions corresponded well to Maxwell–Boltzmann distributions and the temperatures rose from 800 K at a fluence of 0.06 J/cm$^2$ to 3000 K at 0.12 J/cm$^2$. Another stable product that was encountered was CO. Its velocity distribution tended to be more complex than that of MMA because it can be produced not only in the primary UV photon–polymer interaction but also in the process of ionization of the MMA. If the latter contribution is subtracted out, the CO velocities also fitted a Maxwell–Boltzmann distribution which corresponded to the same characteristic temperature as for MMA at that fluence.

As the laser fluence was increased above 0.20 J/cm$^2$, the velocity distribution of MMA was considerably broadened and no longer fitted the Maxwell–Boltzmann equation. There appeared to be both a fast component and a component that fitted the thermal distribution at the same time in the stream of MMA, the former becoming progressively more important with increasing fluence. Note that the quantum yield of MMA also reaches a maximum at about 0.25 J/cm$^2$ in the determination of Srinivasan et al.[30] (Figure 11) and the etch depth/pulse starts to drop off at about this fluence (Figure 2). At first sight, there may appear to be a conflict between the results on velocity distributions of the products from PMMA that were obtained by LIF and from mass spectrometry. Actually, the LIF studies were done with 248-nm photons and the product that was measured, namely $C_2$, is undoubtedly formed by multiphoton reactions as has been pointed out already.

The mass spectrometric studies were carried out at 193 nm and at fluences at which one-photon reactions may prevail. The departure from Maxwell–Boltzmann distributions in the velocities of MMA with increasing fluence would be consistent with multiphoton reactions overtaking one-photon photochemistry. It is very desirable to extend both analytical approaches to wider ranges of wavelengths and fluences.

In addition to velocity distribution measurements that provide information on a so-called translational temperature, it is desirable to have a vibrational–rotational temperature also for the same species. Population distribution in each rotational level of a vibrational transition can be obtained by LIF measurements. The entire vibrational spectrum with its rotational envelope can also be obtained from the emission spectrum of the species. The former approach has so far been limited to UV laser ablation of graphite and sapphire[56] but the latter has been used quite effectively by Davis et al.[12] for the CH molecule that is observed in the plume from the ablation of PMMA with 193-nm pulses. The (0,0), (1,1), and (2,2) bands of the CH $A^2\Delta \rightarrow X^2\Pi$ transition at 431.4 nm were resolved in a vacuum environment. CH was chosen for detailed study since its large rotational constants make its band structure readily rotationally resolvable and its $A^2\Delta \rightarrow X^2\Pi$ transition is spectroscopically well characterized. The experimental spectrum and the computer fit correspond to vibrational and rotational temperatures being in equilibrium at 3200 ± 200 K. The authors conclude that because of the rapid thermalization rates between rotational and thermal motion, the temperature above the ablation zone is also 3200 K. From the photon energy that is expended in etching and the specific heat of PMMA, it is possible to calculate a maximum temperature that is obtainable when all of the photon energy merely heats the substrate. This temperature is only about 1900 K. They therefore deduce that the higher temperature that exists in the plume is a result of exothermic photochemical reactions that are caused by the photons. Reference was made earlier to the work of the same group on velocity measurements on CH molecules in the same system which yielded a translational temperature of about 11 000 K. This is consistent with the idea that in supersonic expansions, the translational temperature would be higher than the vibrational–rotational temperatures. A useful model of the ablation dynamics has been proposed[48] that is consistent with experimental results on the velocity and angular distribution of the ablated material.

## IV. UV Laser Ablation Mechanisms

Controversy over the mechanism of this process stated almost as soon as the first examples were made known in 1982–1983. At that time, there was only one firm observation concerning the interaction of UV laser pulses with polymers. It related to the precision of the etch patterns and the lack of thermal damage to the substrate. Since this observation was on the material that did *not* ablate, it was not the most fruitful approach to the understanding of the chemistry of the material that was ablated. This differentiation between the actions of different lasers of wavelengths ranging from the UV to the infrared became even more tenuous when it became clear that, even in the UV region,

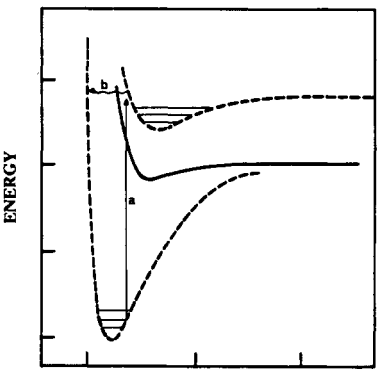


**Figure 19.** Energy-level diagram for hypothetical bond A–B. The lower broken line represents the ground electronic state; the upper broken line and the solid line represent excited states. Reprinted from ref 59; copyright 1986 American Association for the Advancement of Science.

193-nm pulses gave better results than 248-nm pulses, which, in turn, were better than 308-nm pulses. After 7 years of active research by many groups, it is now possible for one to appreciate many of the complexities of UV laser ablation. At the very least, one can eliminate certain mechanistic possibilities with confidence. It also seems likely that a simple, general mechanism that is applicable to all organic solids at all UV wavelengths does not exist. It is hardly surprising that the controversy over the mechanism continues to be a lively subject.[57,58]

There are two aspects to the mechanism by which UV laser pulses bring about the etching of polymer surfaces with a minimum of thermal damage to the substrate. These are (i) the reaction path in which the polymer bonds are actually broken and (ii) a quantitative model of etch behavior as a function of pulse width, wavelength, and fluence. The principal reaction paths that have been proposed can be understood by referring to an energy diagram (Figure 19).[59] It is generally accepted that the absorption of UV photons results in electronic excitation (path a). The excited electronic state can undergo decomposition in that state, which would be a purely photochemical reaction, or, if the excited molecule undergoes internal conversion (path b) to a vibrationally excited ground state, any subsequent decomposition can be considered to be the equivalent of a thermal process. This is the so-called photothermal mechanism in which the photons merely act as a source of thermal energy. Along either pathway the products can be the same (although they do not have to be) and any excess energy over that needed to break the bonds will remain in the products and will be dissipated in the ablated fragments. If the time for ablation is of the order of the duration of the laser pulse (~20 ns), the diffusion of the thermal energy to the unirradiated portion of the substrate will extend to 600 Å in a material with a thermal diffusivity of $4 \times 10^{-4}$ cm/s. Therefore it would be expected that the region showing thermal damage would be negligibly small.

A detailed knowledge of the chemistry of the ablation products is essential in order to construct a reaction pathway for the breakup of the polymer. As has been pointed out in an earlier section, more than one analytical method should be used and a mass balance must be realized. Other critical problems are the possibility that the composition of the products is a function of the

fluence (more strictly, the power density of the laser beam at the polymer surface) and the necessity to avoid the secondary decomposition of the primary products by the tail end of the laser pulse. The first problem has been shown to exist in the ablation of Kapton.[31] The second problem can be inferred to exist from experiments in which the width of the laser pulse was either shortened to picoseconds[60] or even femtoseconds[34,61] or stretched by linking two separate, identical pulses together with a set time delay.[62] Ablation with shortened pulses, especially those of <1-ps duration gives such novel results[63] that the processes involved in this instance may not be same as those obtained with pulses of longer (many nanosecond) duration.

With the exception of PMMA and the silane polymers, there is insufficient analytical evidence in all other cases to construct a chemical reaction pathway that has any experimental basis. On the other hand, there has been no shortage of theories that attempt to describe the etching of a polymer by UV laser pulses.[5,8,34,36,64-72] All of them attempt to calculate the rate at which photon energy is deposited in a volume element that undergoes ablation. Either directly or indirectly, they involve the absorption coefficient of the polymer for the UV wavelength of the laser radiation. Beer's law is assumed to be valid at the power densities that are used to bring about ablation. If this assumption is proved to be invalide, nearly all of these theories will have to be revised.

The expression

$$l_f = \frac{1}{\alpha} \log \frac{F}{F_0} \qquad (1)$$

which relates the etch depth per pulse to the fluence ($F$), the fluence threshold ($F_0$), and the absorptivity ($\alpha$) at that wavelength, has been derived by more than one group.[5,8,65] The derivation merely relates to the deposition of the photon energy according to Beer's law and is independent of the assumed mechanism. This equation can be tested by plotting $l_f$ vs log $F$ when a straight line with a slope of $1/\alpha$ should be obtained. In fact, in many instances there is a linear relationship over a substantial portion of the plot but the slope is not $1/\alpha$. In other cases, the slope is not linear at all over even a small range of fluence. There is no reported example of a polymer whose etch curve fits eq 1 exactly.

Early views of this phenomenon implicitly assumed that ablation followed the deposition of all of the photons of the laser pulse in the solid. Note that in eq 1 there is no time-dependent quantity at all. The photoacoustic experiments mentioned earlier typically showed that, when a fraction of the pulse energy had been deposited in the film, the material started to ablate. The correlation of these data to those obtained by fast UV scanning spectroscopy of the ablating surface and also to a simulation of UV laser ablation was also pointed out.

A knowledge of the time profile of ablation affects the calculations of the temperature rise in the volume of material that ablated. These calculations, which form the basis for the photothermal mechanism, depend strongly upon the time profile of not merely the bond-breaking step (which, presumably, is the signal that is sensed by photoacoustic methods) but the ejection of the fragments that carry away the excess energy of the photon over that needed for bond breaking. This aspect of the ablation phenomenon is just beginning to be probed by using picosecond pulses not only in UV ablation[15] but also in the ablation of polymers by visible lasers.[73] The data that are obtained should give a more detailed picture of the events that occur during one single UV laser pulse of a few nanosecond duration. Analysis of the existing data which consider the etching by a single pulse as a single event in comparison to pyrolysis data (Kapton[37], PMMA[74]) and the discussion it engendered[57,58] will be of historical interest!

The first model that takes into account the changes in the substrate structure even as the laser photons penetrate the material was proposed by Keyes, Clarke, and Isner[68] and subsequently elaborated by Palmer, Keyes, Clarke, and Eisner.[72] The passage of photons will cause chemical bonds to be broken so that the photon intensity at any depth will evolve with time. The time-dependent passage of the laser pulse through the ablating material that is explained in the theory has been adapted by models proposed by others.[34,61,64,70] No prior way to solve the resulting expressions exist and experimental data have been fitted to the model only by the introduction of adjustable parameter(s). This is not necessarily undesirable if the resulting information can be used to predict the behavior of new polymers or of existing polymers under different reaction conditions such as laser pulse width, laser wavelength, introduction of "doping" material, etc. Such is not the case, at least not at the time of the writing of this review.

A key item of the controversy, viz., photochemical vs photothermal mechanism in UV laser ablation of carbon chain polymers, has been settled in a very simple manner in the case of the polysilanes. The "virtual identity of the UV laser desorption and the IR laser pyrolysis mass spectra of poly(*n*-pentylsilane) suggests that under normal fluence conditions even the former process is predominantly photothermal in nature".[24] This is, of course, a very different case from that of a carbon chain polymer such as PMMA in which product compositions change very significantly even in going from 193 to 248 nm.

## V. Current Directions

The interaction of UV laser pulses with polymers continues to be an active field of research. The directions in which work is currently being pursued are as follows:

(i) Variations in the temporal width of the laser pulse have been used, with a view toward making efficient use of the laser photons while maintaining the quality of the etched surface. Pulses varying in their full width at half-maxima from 300 ns[54] to 5 ps[60] to a few hundred femtoseconds[34,61,63,75] have been used, but there is no general agreement on the effect of the pulse width on the ablation process. The data are only preliminary and further experimentation is certainly needed to resolve the issue.

(ii) Intrapulse probing of the polymer to see changes in the absorptivity have been carried out.[34,35,76] Once again, while the results show that the absorption characteristics of the material in the optical path change even in the duration of a 20–30-ns pulse, definitive interpretations are not yet available.

(iii) "Doping" of the polymer with a low molecular weight absorber has been found to promote the ablation sensitivity of a polymer. Several articles have been published on this subject,[46,77-79] and it is undoubtedly a fruitful approach for technological applications.

The technology based on UV laser ablation of polymers has progressed with considerable speed. Reviews[59,80-87] have appeared that give a partial list of the many applications for excimer lasers in general and UV ablation of polymers in particular. The polyimide PMDA-ODA, which in the form of Kapton film finds wide use as an insulator as well as a thermally resistant film, lends itself well to ablative etching by UV lasers. The results obtained with UV laser radiation at 308 nm (the most favored wavelength for industrial applications) are superior to those obtained in the near-IR (Nd:YAG laser) or mid-IR ($CO_2$ laser).[80] But practical problems, principally with the solid debris that is the product of ablation, exist.[88] Ablative patterning of acrylate polymer films and polysilane films has been shown to be feasible, but the current trend is still to use the excimer laser merely as a conventional light source for the exposure of deep-UV photoresists. The acceptance of the excimer laser as an industrial tool will be a slow process mainly because of cost and reliability considerations.

## VI. References


(1) Zandee, L.; Bernstein, R. B. *J. Chem. Phys.* **1979**, *70*, 2574; *1979*, *71*, 1359.
(2) Koplitz, B. D.; McVey, J. *J. Phys. Chem.* **1985**, *89*, 4196.
(3) Srinivasan, R.; Mayne-Banton, V. *Appl. Phys. Lett.* **1982**, *41*, 576.
(4) Srinivasan, R.; Leigh, W. J. *J. Am. Chem. Soc.* **1982**, *104*, 6784.
(5) Deutsch, T. F.; Geis, M. W. *J. Appl. Phys.* **1983**, *54*, 7201.
(6) Geis, M. W.; Randall, J. N.; Deutsch, T. F.; Efremow, N. N.; Donnelly, J. P.; Woodhouse, J. D. *J. Vac. Sci. Technol.* **1983**, *B1*, 1178.
(7) Kawamura, Y.; Toyoda, K.; Namba, S. *Appl. Phys. Lett.* **1982**, *40*, 374.
(8) Andrew, J. E.; Dyer, P. E.; Forster, D.; Key, P. H. *Appl. Phys. Lett.* **1983**, *43*, 717.
(9) Trokel, S. T.; Srinivasan, R.; Braren, B. *Am. J. Ophthalmol.* **1983**, *96*, 710.
(10) Koren, G.; Yeh, J. T. C. *Appl. Phys. Lett.* **1984**, *44*, 1112.
(11) Koren, G.; Yeh, J. T. C. *J. Appl. Phys.* **1984**, *56*, 2120.
(12) Davis, G. M.; Gower, M. C.; Fotakis, C.; Efthimiopoulos, T.; Argyrakis, P. *Appl. Phys.* **1985**, *A36*, 27.
(13) Dyer, P. E.; Srinivasan, R. *Appl. Phys. Lett.* **1986**, *48*, 445.
(14) Srinivasan, R.; Dyer, P. E.; Braren, B. *Lasers Surg. Med.* **1987**, *6*, 514.
(15) Simon, P. *Appl. Phys. B* **1989**, *48*, 253.
(16) Gorodetsky, G.; Kazyaka, T. G.; Melcher, R. L.; Srinivasan, R. *Appl. Phys. Lett.* **1985**, *46*, 828.
(17) Srinivasan, R.; Braren, B.; Dreyfus, R. W. *J. Appl. Phys.* **1987**, *61*, 372.
(18) Yeh, J. T. C. *J. Vac. Sci. Technol. A* **1986**, *4*, 653.
(19) Cole, H. S.; Liu, Y. S.; Philipp, H. R. *Appl. Phys. Lett.* **1986**, *48*, 76.
(20) Lazare, S.; Srinivasan, R. *J. Phys. Chem.* **1986**, *90*, 2124.
(21) Srinivasan, R.; Lazare, S. *Polymer* **1985**, *26*, 1297.
(22) Lazare, S.; Hoh, P. D.; Baker, J. M.; Srinivasan, R. *J. Am. Chem. Soc.* **1984**, *106*, 4288.
(23) Lazare, S.; Srinivasan, R. *Proceedings of the 2nd International Conference of Polyimides*; Society of Plastics Engineers: Ellenville, NY, 1985; p 407.
(24) Magnera, T. F.; Balajii, V.; Michl, J.; Miller, R. D.; Sooriyakumaran, R. *Macromolecules* **1989**, *22*, 1624.
(25) Magnera, T. F.; Balaji, V.; Michl, J. *Silicon Chemistry*; Ellis Horwood Publishers: Chichester, England, 1988; Chapter 4,5.
(26) Miller, R. D.; Hofer, D.; Fickes, G. N.; Willson, C. G.; Marinero, E. E.; Trefonas, P.; West, R. *Polymn. Eng. Sci.* **1986**, *26*, 1129.
(27) Miller, R. D.; Hofer, D.; Rabolt, J. F.; Sooriyakumaran, R.; Willson, C. G.; Fickes, G. N.; Guillet, J. E. *Polymers for High Technology: Electronics and Photonics*; ACS Symp. Ser. No. 346; American Chemical Society: Washington, DC, 1987, Chapter 15.
(28) Ziegler, J. M.; Harrah, L. A.; Johnson, A. W. *Proc. SPIE* **1985**, *539*, 166.
(29) Hofer, D. C.; Jain, K.; Miller, R. D. *IBM Tech. Discl. Bull.* **1984**, *26*, 5683.
(30) Srinivasan, R.; Braren, B.; Seeger, D. E.; Dreyfus, R. W. *Macromolecules* **1986**, *19*, 916.
(31) Estler, R. C.; Nogar, N. S. *Appl. Phys. Lett.* **1986**, *49*, 1175.
(32) Gupta, A.; Llang, R.; Tsay, F. D.; Moacanin, J. *Macromolecules* **1980**, *13*, 1696.
(33) Kuper, S.; Stuke, M. *Appl. Phys.* in press.
(34) Kuper, S.; Stuke, M. *Appl. Phys.* **1987**, *B44*, 199.
(35) Davis, G. M.; Gower, M. C. *J. Appl. Phys.* **1987**, *61*, 2090.
(36) Brannon, J. H.; Lankard, J. R.; Baise, A. I.; Burns, F.; Kaufman, J. *J. Appl. Phys.* **1985**, *58*, 2036.
(37) Sroog, C. E. *J. Polym. Sci., Macromol. Rev.* **1976**, *11*, 186.
(38) Creasy, W. R.; Brenna, J. T. *Chem. Phys.* **1988**, *126*, 453.
(39) Otis, C. E. *Appl. Phys.*, in press.
(40) von Gutfeld, R. J.; Srinivasan, R. *Appl. Phys. Lett.* **1987**, *51*, 15.
(41) Taylor, R. S.; Leopold, K. E.; Singleton, D. L.; Paraskevopoulos, G.; Irwin, R. S. *J. Appl. Phys.* **1988**, *64*, 2815.
(42) Singleton, D. L.; Paraskevopoulos, G.; Irwin, R. S. *J. Appl. Phys.*, in press.
(43) Dyer, P. E.; Jenkins, S. D.; Sidhu, J. *Appl. Phys. Lett.* **1986**, *49*, 453.
(44) Danielzik, B.; Fabricius, N.; Rowekamp, M.; von der Linde, D. *Appl. Phys. Lett.* **1986**, *48*, 212.
(45) Feldmann, D.; Kutzner, J.; Laukemper, J, et al. *Appl. Phys. B* **1987**, *44*, 81.
(46) Srinivasan, R.; Braren, B.; Dreyfus, R. W.; Hadel, L.; Seeger, D. E. *J. Opt. Soc.* **1986**, *A3*, 785.
(47) Larciprete, R.; Stuke, M. *Appl. Phys. B* **1987**, *42*, 181.
(48) Garrison, B. J.; Srinivasan, R. *Appl. Phys. Lett.* **1984**, *44*, 849.
(49) Garrison, B. J.; Srinivasan, R. *J. Appl. Phys.* **1985**, *57*, 2909.
(50) Garrison, B. J.; Srinivasan, R. *J. Vac. Sci. Technol.* **1985**, *A3*, 746.
(51) Hansen, S. G. Conference on Lasers and Electro-optics, Baltimore, 1989.
(52) Srinivasan, R.; Dreyfus, R. W. *Laser Spectroscopy VII*; Springer-Verlag: Berlin, 1985.
(53) Dyer, P. E.; Sidhu, J. *J. Appl. Phys.*, in press.
(54) Taylor, R. S.; Singleton, D. L.; Paraskevopoulos, G. *Appl. Phys. Lett.* **1987**, *50*, 1779.
(55) Utterback, N. G.; Tang, S. P.; Friichtenicht, J. F. *Phys. Fluids* **1976**, *19*, 900.
(56) Dreyfus, R. W.; Kelly, R.; Walkup, R. E.; Srinivasan, R. *SPIE Excimer Lasers and Optics* **1987**, *48*, 212.
(57) Dijkkamp, D.; Gozdz, A. S.; Venkatesan, T.; Wu, X. D. *Phys. Rev. Lett.* **1987**, *58*, 2142.
(58) Srinivasan, R. *Phys. Rev. Lett.* **1988**, *60*, 381.
(59) Srinivasan, R. *Science* **1986**, *234*, 559.
(60) Nikolaus, B. Conference on Lasers and Electro-optics, San Francisco, 1986.
(61) Srinivasan, R.; Sutcliffe, E.; Braren, B. *Appl. Phys. Lett.* **1987**, *51*, 1285.
(62) Srinivasan, R.; Braren, B. *Appl. Phys. Lett.* **1988**, *53*, 1233.
(63) Kuper, S.; Stuke, M. *Appl. Phys. Lett.* **1989**, *54*, 4.
(64) Mahan, G. D.; Cole, H. S.; Liu, Y. S.; Philipp, H. R. *Appl. Phys. Lett.* **1988**, *53*, 2377.
(65) Srinivasan, R.; Braren, B. *J. Polym. Sci., Polym. Chem. Ed.* **1984**, *22*, 2601.
(66) Jellinek, H. H. G.; Srinivasan, R. *J. Phys. Chem.* **1984**, *88*, 3048.
(67) Melcher, R. L. *Laser Processing and Diagnostics*; Springer-Verlag: Berlin, 1984; p 418.
(68) Keyes, T.; Clarke, R. H.; Isner, J. M. *J. Phys. Chem.* **1985**, *89*, 4194.
(69) Srinivasan, V.; Smrtic, M. A.; Babu, S. V. *J. Appl. Phys.* **1986**, *59*, 3861.
(70) Sutcliffe, E.; Srinivasan, R. *J. Appl. Phys.* **1986**, *60*, 3315.
(71) Kiss, L. B.; Simon, P. *Solid State Commun.*, in press.
(72) Palmer, B. J.; Keyes, T.; Clarke, R. H.; Isner, J. M. *J. Phys. Chem.*, in press.
(73) Kim, H.; Postlewaite, J. C.; Zyung, T.; Dlott, D. D. *J. Appl. Phys.* **1988**, *64*, 2955.
(74) Jellinek, H. H. G.; Luh, M. D. *Makromol. Chem.* **1968**, *115*, 89.
(75) Chuang, M. C.; Tam, A. C. *J. Appl. Phys.* **1989**, *65*, 2591.
(76) Koren, G. *Appl. Phys. Lett.* **1987**, *50*, 1030.
(77) Masuhara, H.; Hiraoka, H.; Domen, K. *Macromolecules* **1987**, *20*, 450.
(78) Hiraoka, H.; Chuang, T. J.; Masuhara, H. *J. Vac. Sci. Technol. B* **1988**, *6*, 463.
(79) Srinivasan, R.; Braren, B. *Appl. Phys. A* **1988**, *45*, 289.
(80) Znotins, T.; Poulin, D.; Reid, J. *Laser Focus* **1987**, May.
(81) Poulin, D.; Eisele, P.; Znotins, T. *Indust. Laser Rev.* **1989**, *4*, 4.

(82) Davis, G. M.; Gibson, A. F.; Gower, M. C.; Moody, R. A. *Microcircuit Eng.* **1983**, *83*, 191.
(83) Davis, G. M.; Gower, M. C. *IEEE Electron Device Lett.* **1986**, *EDL-7*, 543.
(84) Lazare, S.; Granier, V.; Lutgen, P.; Feyder, G. *Rev. Phys. Appl.* **1988**, *23*, 1065.
(85) Miller, R. D.; Hofer, D.; Mckean, D. R.; Willson, C. G.; West, R.; Trefonas, P. T. *Materials for Microlithography: Radiation-Sensitive Polymers* ACS Symp. Ser 266; American Chemical Society: Washington, DC, 1984; Chapter 14.
(86) Miller, R. D.; Macdonald, S. A. *J. Imaging Sci.* **1987**, *31*, 43.
(87) Rice, S.; Jain, K. *Appl. Phys. A.* **1984**, *33*, 195.